

Local Distribution of Biomolecules on Biosensing Surfaces Investigated by Scanning Force Microscopy

W. HUBER,* T. RICHMOND,† D. ANSELMETTI,† D. SCHLATTER,*
M. DREIER,† J. FROMMER† AND H.-J. GÜNTHERODT†

**F. Hoffmann-La Roche Ltd, Pharmaceutical Research New Technologies,
CH-4002 Basel, Switzerland, †Institute of Physics, University of Basel,
Klingelbergstrasse 82, CH-4056 Basel, Switzerland*

Systematic imaging of biological macromolecules such as protein A or h-IgG on optical sensor surfaces has been performed using scanning force microscopy (SFM). The SFM measurements provided information on the spatial distribution of biologically active species bound or adsorbed to the surface. They were also used to determine quantitatively the equilibrium surface coverage which is reached in contact with a solution containing a given concentration of biologically active species. These values are compared with the respective values determined by optical surface sensitive measurements.

KEYWORDS: biological macromolecules, distribution, biosensors, SFM

INTRODUCTION

The potential of biosensors as a future tool for bioanalytical tests in human diagnostics, environment analysis, food and drink control, and biofunctional research is well accepted (Camman *et al.*, 1991; Thompson & Krull, 1991; Wong *et al.*, 1991). However, practical applications of such biosensors are still uncommon. The present impasse with this promising technology is well known, i.e. the preparation of a sample–sensor interface which exhibits a high affinity and selectivity for the analyte molecule of interest (Alvarez-Icaza & Bilitewsky, 1993). The affinity and selectivity of the interface is generated by the immobilization of biologically recognizing molecules on the surface of the sensor. However, immobilization causes problems regarding the homogeneity of the surface coverage, the density and the orientation of the biomolecules.

Recently, we have described optical immunosensors which exhibit extremely high sensitivities, even in undiluted human serum. Anti h-IgG was detected in buffer solution down to a concentration of 1×10^{-11} M and hepatitis B surface antigen in human serum down to a concentration of 2×10^{-13} M (Huber *et al.*, 1992; Schlatter *et al.*, 1993). It has been claimed that the exceptional performance of these optical

Correspondence should be addressed to D. Anselmetti. Present address: CIBA-GEIGY LTD, Research Services, Physics, CH-4002 Basel, Switzerland.

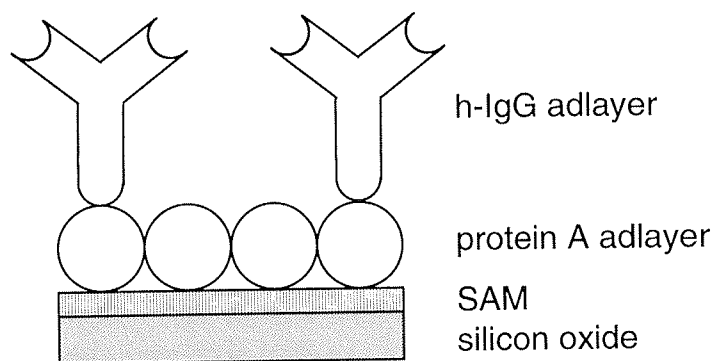


FIGURE 1. Schematic drawing of the multi-layered structure of the sensor surface.

immunosensors is partly due to the sensitivity of the optical transducers used and also to the appropriate immobilization of the recognizing biomolecules on the transducers' surface. A schematic drawing of the multi-layered structure of the sensitive interface prepared on the optical transducers is given in Figure 1. The $\text{SiO}_2/\text{TiO}_2$ surface of the optical transducer is first modified with a self-assembled monolayer (Ulman, 1990) to which a monolayer of protein A is covalently attached. This monolayer has the ability to bind IgG molecules covalently via their F_c domain (Goding, 1978) forming a second protein layer of closely packed and properly aligned antibodies. The nature of the monolayer and the proper distribution of the proteins within such protein adlayers on these optical transducers has so far not been demonstrated. A possibility of obtaining information about the distribution of biomolecules on surfaces is electron or fluorescence microscopy. However, both methods have the disadvantage that for detection, the molecules have to be modified, e.g. by staining or fluorescence labelling. Surface analytical techniques which give direct information on the distribution and orientation of biomolecules, without modification of the molecules such as local probe methods, are not as yet fully established. Recent investigations with local probe techniques have shown that these methods have the potential to generate resolved pictures of surfaces derivatized with biomolecules (Butt *et al.*, 1990; Hansma *et al.*, 1993).

In this study, we investigate the above-mentioned protein adlayers and, in addition, a test system consisting of anti-protein A-coated gold spheres, by scanning force microscopy (SFM). Our results demonstrate the usefulness of this technique for investigating the local density and the distribution of immobilized biomolecules on sensor surfaces. The results of such local probe investigations can be correlated with the results obtained by optical sensor techniques.

EXPERIMENTAL

Substrate Material

The chemical and biochemical adlayers were prepared either on silicon wafers with a 1 nm thick SiO_2 layer (Wacker-Chemitronic GmbH) or on $\text{SiO}_2/\text{TiO}_2$ sol-gel wave guides prepared on AF45 float glass according to the literature (Lukosz & Tiefenthaler, 1983) using Liquicoat TISI 4030 (Merck). Similar images of modified surfaces were observed for the different inorganic substrate materials. However, as the roughness of the $\text{SiO}_2/\text{TiO}_2$ was found to be slightly higher than that of the SiO_2 on silicon wafers, for the purpose of imaging, organic and biochemical adlayers were deposited on the SiO_2 surface of silicon wafers.

Chemicals and Reagents

Ethylchloroformate, *N*-hydroxysuccinimide, protein A and h-IgG were from Fluka. Monoclonal anti-protein A (Clone SPA-27) was from Sigma. The preparation of gold particles (12 nm in diameter) and the coating of these gold particles with anti-protein A was carried out according to procedures described in the literature (Slot & Geuze, 1985; Keifer *et al.*, 1986). 11-(Dimethylchlorosilyl)-undecanoylchloride was synthesized according to established procedures.

Pre-treatment of the Surfaces

The substrate surfaces were treated for 15 min with concentrated sulphuric acid and then extensively rinsed with pure water. After this treatment the surfaces were fully wettable with water.

Preparation of the Organic and Biological Adlayers

For the immobilization of protein A the surfaces were chemically modified as follows. In a first step, the surface was treated with a solution of 11-(dimethylchlorosilyl)-undecanoylchloride in CCl_4 (0.05% v/v) for 25 min. The surfaces were then washed with CCl_4 and dried in a jet of nitrogen. By using photoelectron spectroscopy (XPS), it was found in accordance with the literature that the surface mass coverage obtained by this treatment corresponds to the coverage of the surface with a monolayer of undecanoylchloride.

The carboxylic acid groups introduced by this procedure were converted into *N*-hydroxysuccinimide derivatives by the treatment of the surface with a solution of ethylchloroformate (5% v/v) in CH_2Cl_2 /pyridine (20/1 v/v) for 1 h and afterwards for 30 min with a solution of *N*-hydroxysuccinimide (0.5 M) in pyridine.

The surface with the activated carboxylic acid groups was brought into contact with an aqueous buffered solution (acetate buffer, 0.01 M, pH = 5.5) of protein (0.1 mg ml⁻¹) for 1 h. This procedure leads to a covalent attachment of the protein through formation of an amide bond between the carboxylic acid group of the organic adlayer and the free amino groups on the surface of the protein.

The antibody adlayer was formed on this protein A layer by placing the surface in contact for 1 h with a solution containing different concentrations of antibody in phosphate-buffered saline (PBS: 150-mM NaCl, 50-mM Na_2HPO_4 , pH = 7.2).

The adlayer consisting of antibody-coated gold particles was formed by contacting this surface for 1 h with a solution containing different concentrations of coated gold particles in PBS.

Instrumentation

The optical read-out system which was used to monitor the immobilization of protein A and the adsorption of IgG antibodies to this adlayer is described in detail elsewhere (Huber *et al.*, 1992). The instrument measures the input coupling angle of an optical grating coupler sensor, which changes upon the adsorption and desorption of molecules. This change in coupling angle is converted into a change in surface coverage using a linear relationship (Lukosz, 1991). A commercial scanning force microscope equipped with a fluid cell (Digital Instruments, Santa Barbara, CA) was used to investigate the different sample surfaces. The most reproducible results were obtained by measuring the samples in a mixture of ethanol (90%) and nanopure water. Submersing the tip in liquid greatly reduces the interaction forces mainly due

to capillary condensation, allowing a gentle rastering of the tip over the surface at a very low interaction force (e.g. in the order of 10^{-11} N) (Drake *et al.*, 1989). Maintaining a very low force is particularly important in imaging of biomolecules (Weisenhorn *et al.*, 1991). We used silicon nitride cantilevers with spring constants of $0.1\text{--}0.2$ N m $^{-1}$ (Digital Instruments, Santa Barbara, CA and Park Scientific Instruments, Mountain View, CA). When operated at the lowest loading, i.e. at the point just before the tip lifts off from the sample, reproducible imaging of biomolecules with no significant difference regarding cantilever type was possible.

RESULTS AND DISCUSSION

The Silanized Surface

It has been shown that the treatment of hydrophilic SiO $_2$ surfaces with long chain chloroalkylsilanes leads to the formation of well-ordered alkyl monolayers which are covalently linked to the SiO $_2$ backbone (Ulman, 1990). The monolayer structure of these films has been proven by using ellipsometric measurements or photoelectron spectroscopy (Kallury *et al.*, 1992). The monolayer nature of the adlayers generated by treating the SiO $_2$ surface of the silicon wafers with 11-(dimethylchlorosilyl)-undecanoylchloride was proven in our case with XPS. Thereby, we made use of the treatment of the attenuation lengths of the photoelectrons determined by Bain and Whitesides (1989) for a self-assembled monolayer on gold. Assuming this attenuation constant, the thickness of the adlayer formed by the treatment with 11-(dimethylchlorosilyl)-undecanoylchloride was determined to be $1.0 (\pm 0.1)$ nm. This value is slightly smaller than the thickness one would expect for a monolayer consisting of closely packed fully extended C $_{11}$ alkyl chains oriented perpendicularly to the surface. The discrepancy could be explained by the presence of the two methyl groups on the Si atom, which does not allow a very close packing of the alkyl chains. It has been demonstrated using IR spectroscopy (Nuzzo *et al.*, 1987; Tillman *et al.*, 1988; Ulman *et al.*, 1989) that such a reduction in packing density in self-assembled monolayers is usually compensated for by tilting the molecules relative to the surface normal.

Figure 2(a) shows a SFM image of the unmodified SiO $_2$ surface of the cleaned silicon wafer. The roughness of the surface was found to be less than 0.3 nm (the rms calculation was carried out on an area of 500×500 nm 2 with a resolution of 400×400 points). Figure 2(b) depicts the SFM image of the same surface after treatment with (dimethylchlorosilyl)-undecanoylchloride. Direct comparison of the two images indicates a homogeneously distributed organic adlayer as deposited on the whole surface by the silanization procedure. There is no indication of cluster formation by the silanizing reagent. The calculated rms roughness of 0.4 nm is close to the value of the bare surface.

Summarizing the results of XPS and SFM, one can straightforwardly conclude that the adlayer formed by silanization is a closely packed monolayer. Molecular resolution as achieved by SFM, show corrugations of 3 ± 1 Å within the relatively ordered regions of the silanized surface (Figure 2(c)), but no long-range order was observed as might have been expected due to the possible self-ordering of the molecules.

The Protein A Adlayer

The immobilization of protein A on the surface containing activated carboxylic acid groups was monitored using a grating coupler sensor. Figure 3(a) depicts the time-dependent change in surface mass coverage, which was determined by monitoring the

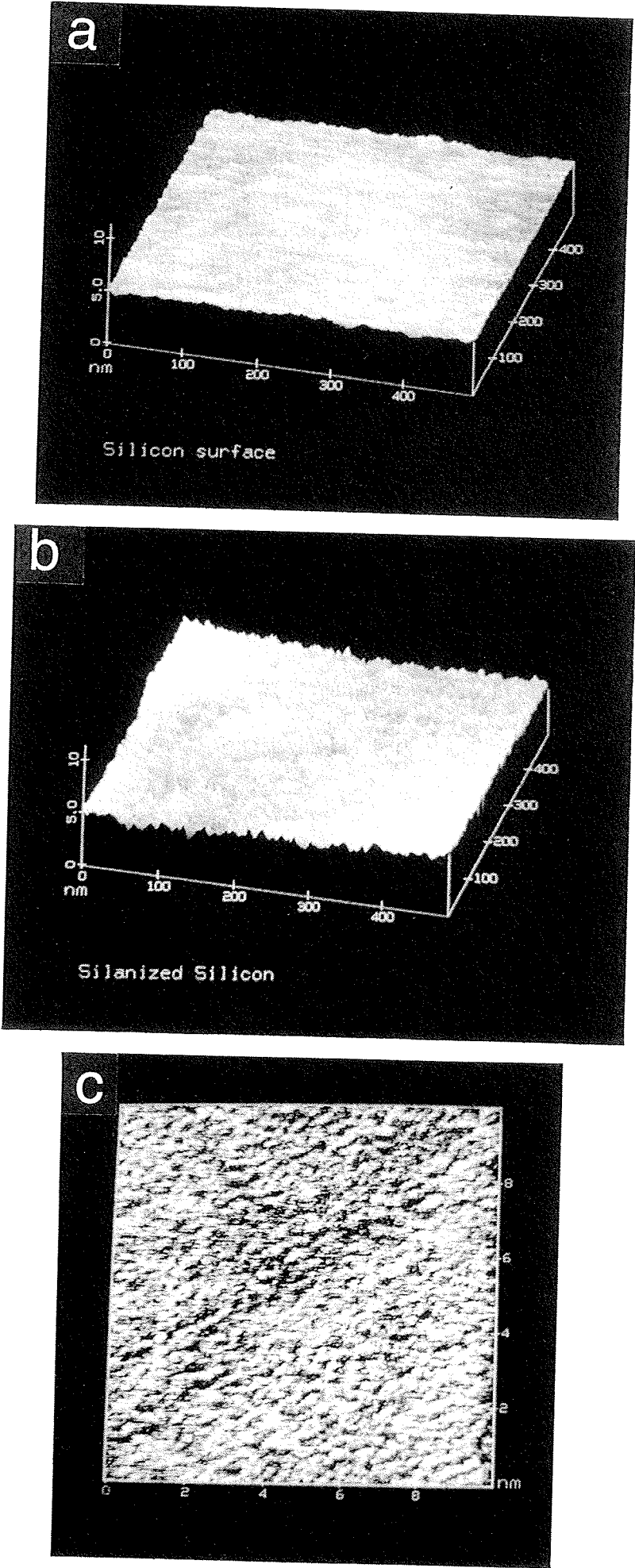


FIGURE 2. SFM images of (a) silicon substrate (b) silanized surface and (c) constant-height mode image of the silanized surface with molecular resolution.

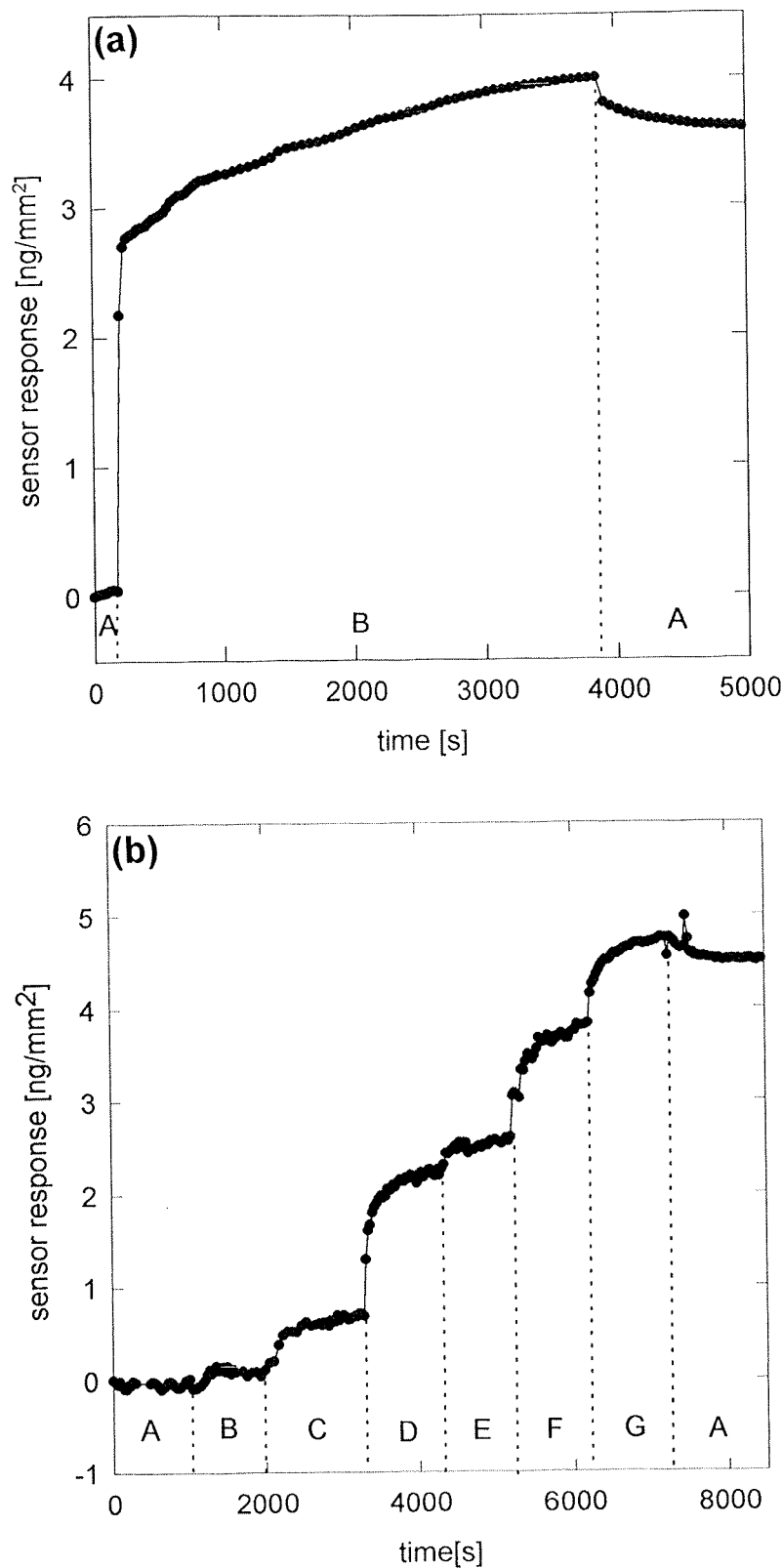


FIGURE 3. (a) Time-dependent change of the surface coverage recorded with the sensor in contact with a protein A solution (concentration = 1 mg ml⁻¹). (b) Time-dependent change of the sensor response during subsequent contacts of a sensor surface carrying protein A with solutions containing increasing amounts of h-IgG: A, buffer; B, 10-nM h-IgG; C, 50-nM h-IgG; D, 500-nM h-IgG; E, 1- μ M h-IgG; F, 100- μ M h-IgG; G, 300- μ M h-IgG.

change in the coupling angle of the TE (transverse electric) mode of the grating coupler and by converting these angular changes to surface mass coverage changes using a relationship established by Lukosz (1991) and Lukosz and Tiefenthaler (1988). At saturation, 3.5 ng mm^{-2} protein A is immobilized on the surface. This value has to be compared with the mass of an ideal closely packed monolayer of protein A, which is calculated by considering the size and shape of the molecule. Protein A is spherical in shape with a radius of approximately 2.5 nm. For a close packing of these spheres the density of protein A is simply $1/(2\sqrt{3}Lr^2) \text{ mol mm}^{-2}$ giving $7.7 \times 10^{-14} \text{ mol mm}^{-2}$, where L denotes the Loschmidt number. Considering the molecular weight of protein A as being 42000 g mol^{-1} , the mass of a closely packed protein A monolayer is calculated to be 3.2 ng mm^{-2} . By comparing this theoretical value with the value obtained from the measurements with the optical sensor, one would expect that the surface is covered with approximately 100% protein A. However, this comparison of a theoretical and a measured surface mass coverage cannot answer questions regarding local properties of the protein A adlayer. Whether the proteins are clustered or homogeneously distributed on the surface can only be addressed using a surface analytical technique with local resolution capabilities. Figure 4 depicts images of the protein A adlayer generated by SFM measurements in contact mode under fluid (Figure 4(a)) and by dynamic force microscopy (DFM) (Figure 4(b)). In DFM the cantilever is driven close to its resonance frequency (typically 150–500 kHz by 1–3 nm). Upon approaching the cantilever towards the surface, the oscillation amplitude is reduced by force gradients and/or damping effects, which are detected with the rectifier or lock-in technique. This method allows a contact-free subtle investigation of soft samples with a minimized force interaction. For more details see Anselmetti *et al.* (1994). From a comparison of these images with the silanized surface of Figure 2(b), the change in surface morphology due to the immobilization of protein A becomes clearly obvious. The homogeneous distribution of spherical features, which are absent on the silanized surface, is indicative of the coverage of the surface with protein A. The diameter of the spherical features is in the order of 35 ± 5 and $6 \pm 2 \text{ nm}$ in Figures 4(a) and (b), respectively. The corresponding corrugation was determined to be 6 ± 2 and $2 \pm 0.5 \text{ nm}$ suggesting a much lower tip-sample interaction in dynamic force microscopy. Due to the finite size of the tip which is in the order of 10–20 nm, imaging of objects of comparable size always suffers from tip geometry contributions. Disregarding possible tip geometry contributions for an estimate of the protein A surface coverage, we find an almost densely packed overlayer with a coverage of $>90\%$. However, the above-mentioned uncertainties as yet do not allow a more accurate calculation.

The Adsorption of IgG on Protein A

The amount of h-IgG adsorbing on such a protein A layer was determined using a grating coupler sensor, the surface of which was modified with the protein A layer. Figure 3(b) depicts the time-dependent change in surface mass coverage when the surface is brought subsequently into contact with buffer solutions containing increasing amounts of h-IgG. This change in surface coverage was again determined by measuring the time-dependent change of the incoupling angle of the TE mode of the grating coupler and by converting this angular change into a change in surface mass. This calculated surface mass change is given on the left-hand side of the graph in Figure 3(b). No surface mass increase could be detected in contact with solutions with a h-IgG concentration below 10 nM. For concentrations above 10 nM the surface loading approaches an equilibrium value for each concentration. Complete occupancy of all potential binding sites on protein A occurred at concentrations above

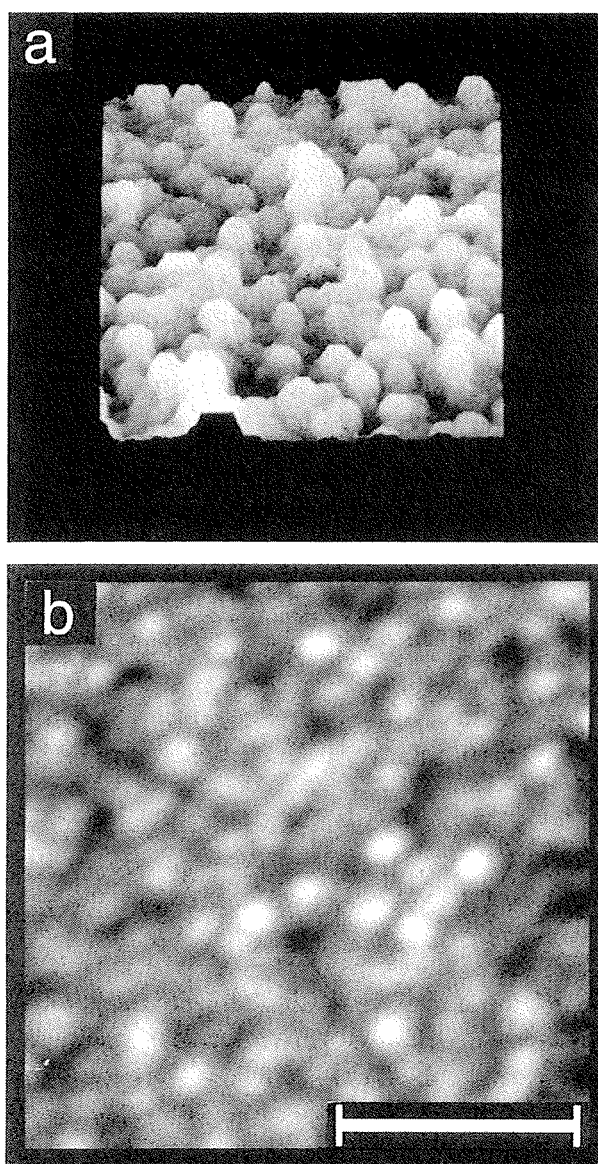


FIGURE 4. Protein A surface as imaged by (a) SFM (image size: $270\text{ nm} \times 270\text{ nm}$) and (b) dynamic force microscopy (the scale bar corresponds to 50 nm).

approximately $300\text{ }\mu\text{m}$. The mass coverage which corresponds to this saturation is 4.5 ng mm^{-2} . This value can be compared with the estimated mass of a closely packed monolayer of h-IgG molecules. Based on geometrical arguments (Essers, 1988), this mass is calculated to be $1.5\text{--}6.5\text{ ng mm}^{-2}$ depending on the orientation (lying and upright positions) of the molecules on the surface. Comparing these theoretical values with the value determined with the optical sensor, one may assume that a closely packed monolayer of h-IgG molecules is formed on top of the protein A adlayer with the h-IgG molecules oriented preferentially with their long axis perpendicular to the surface.

Figures 5(a)–(d) are SFM images of surfaces of protein A brought into contact with solutions containing 0 and 50 nM and 1 and $10\text{ }\mu\text{M}$ h-IgG, respectively. The images qualitatively agree with the sensor measurements as the brighter, i.e. taller objects, increase in concentration from Figures 5(a)–(d). Within most parts of the images in Figures 5(a) and (b), i.e. those with the lowest concentrations of IgG present, the same spherical features of $35 \pm 5\text{ nm}$ in diameter and corrugation of $6 \pm 2\text{ nm}$ as in Figure 4 are visible. In Figure 5(d), these are replaced with objects of $80 \pm 10\text{ nm}$ in diameter and $15 \pm 5\text{ nm}$ in height. As mentioned above, there are errors involved due to the finite size of the tip which influence the observed lateral size of the molecules. In the present case, as h-IgG molecules are supported by a bed of soft

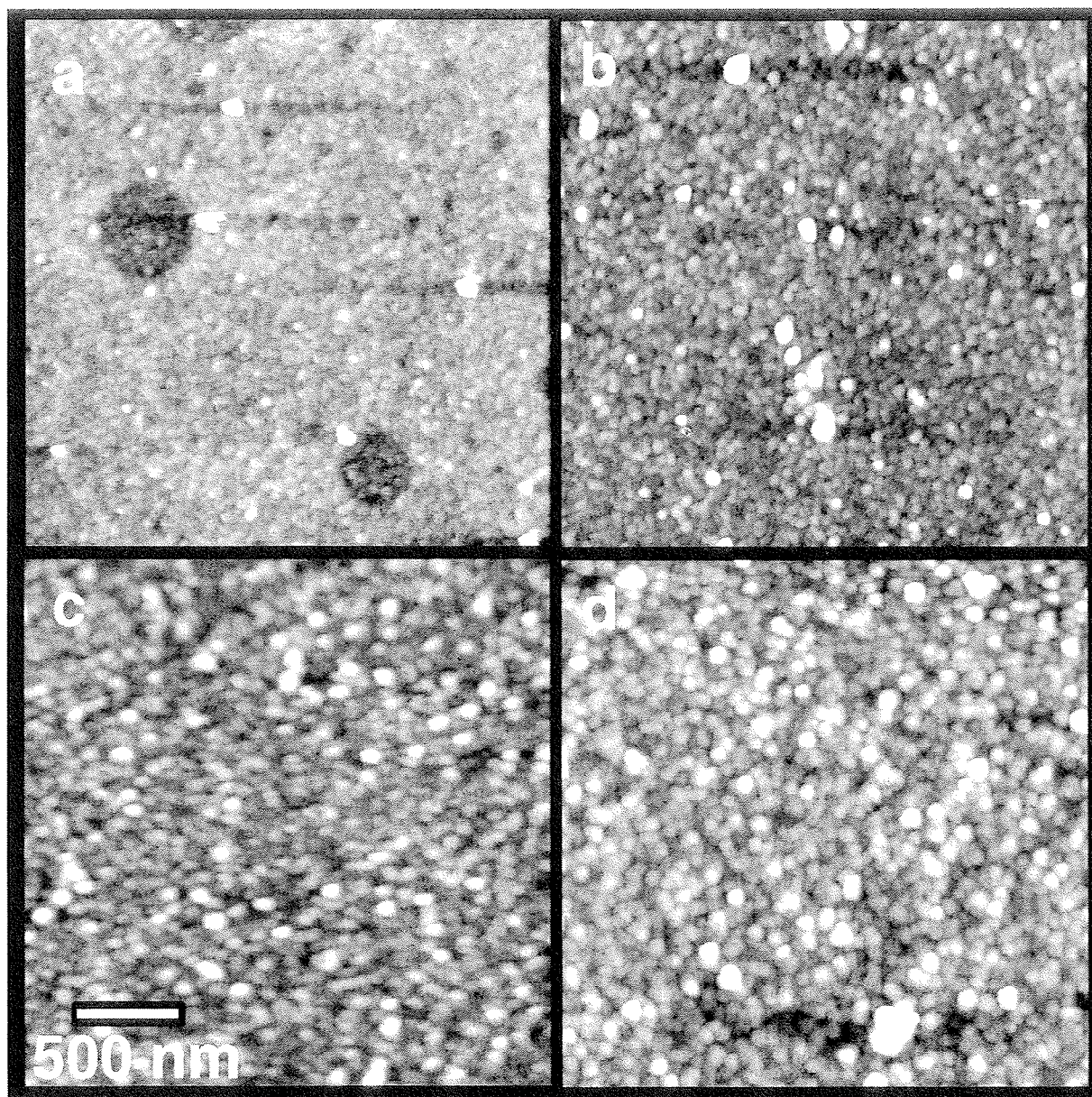


FIGURE 5. Successive increase in surface coverage of h-IgG antibodies on a protein A surface as measured by SFM.

proteins, a further error arises in detection of the molecules as the force of the cantilever pushes the IgG molecules into the background. An estimation of the coverage of the surfaces by h-IgG by integrating over pixels with heights of over 6 nm, giving 0.8 ± 0.3 , 3.5 ± 1 , 40 ± 8 and $80 \pm 15\%$ coverage compared to sensor calculations of 0, 15, 58 and 81%. For these estimates, we always imaged several different surface areas ($>1 \mu\text{m}^2$) typically containing 10–1000 macromolecules (depending on the molecular surface concentration).

The Adsorption of Gold Particles Coated with Anti-protein A Antibodies to Protein A Surfaces

In order to enhance the contrast between the protein A adlayer and a second adlayer formed by affinity binding, the above-mentioned protein A layer was placed in contact with different solutions containing different concentrations of colloidal gold particles coated with anti-protein A antibodies. It has been proven with optical sensor methods that the adsorption behaviour of these gold particles parallels the behaviour of the h-

IgG molecules as already described above. Surfaces have been chosen for SFM measurements for which the sensor response (assuming a linear relationship between surface coverage and sensor signal) is indicative of surface coverages of 1, 20, 50 and 100%. Figure 6 depicts the SFM images obtained from such surfaces. The integration over pixels of the images in Figures 6(a)–(d) which measure more than 5 nm in height shows a coverage of the surface by gold complexes of 0.6 ± 0.3 , 3 ± 1 , 22 ± 2 and $94 \pm 5\%$, respectively. So the measurements seem to underestimate the surface coverage relative to the sensor response at least within the medium concentration range.

CONCLUSION

The idea of combining optical and local probe methods is a relatively new one (Schmitt *et al.*, 1991; Extrand *et al.*, 1993). The present study compares results concerning surface coverage, extracted using a local probe method (SFM) and those from an integrating surface analytical technique (evanescent wave measurements). Both techniques can be used to determine quantitatively the surface coverage of a planar optical wave guide with biologically active molecules (protein A, h-IgG) or particles (antibody-coated gold spheres). A good correlation of the results from the two techniques is only found at high surface coverage (50%). At low coverages, SFM underestimates or the optical measurements overestimate the “true” surface

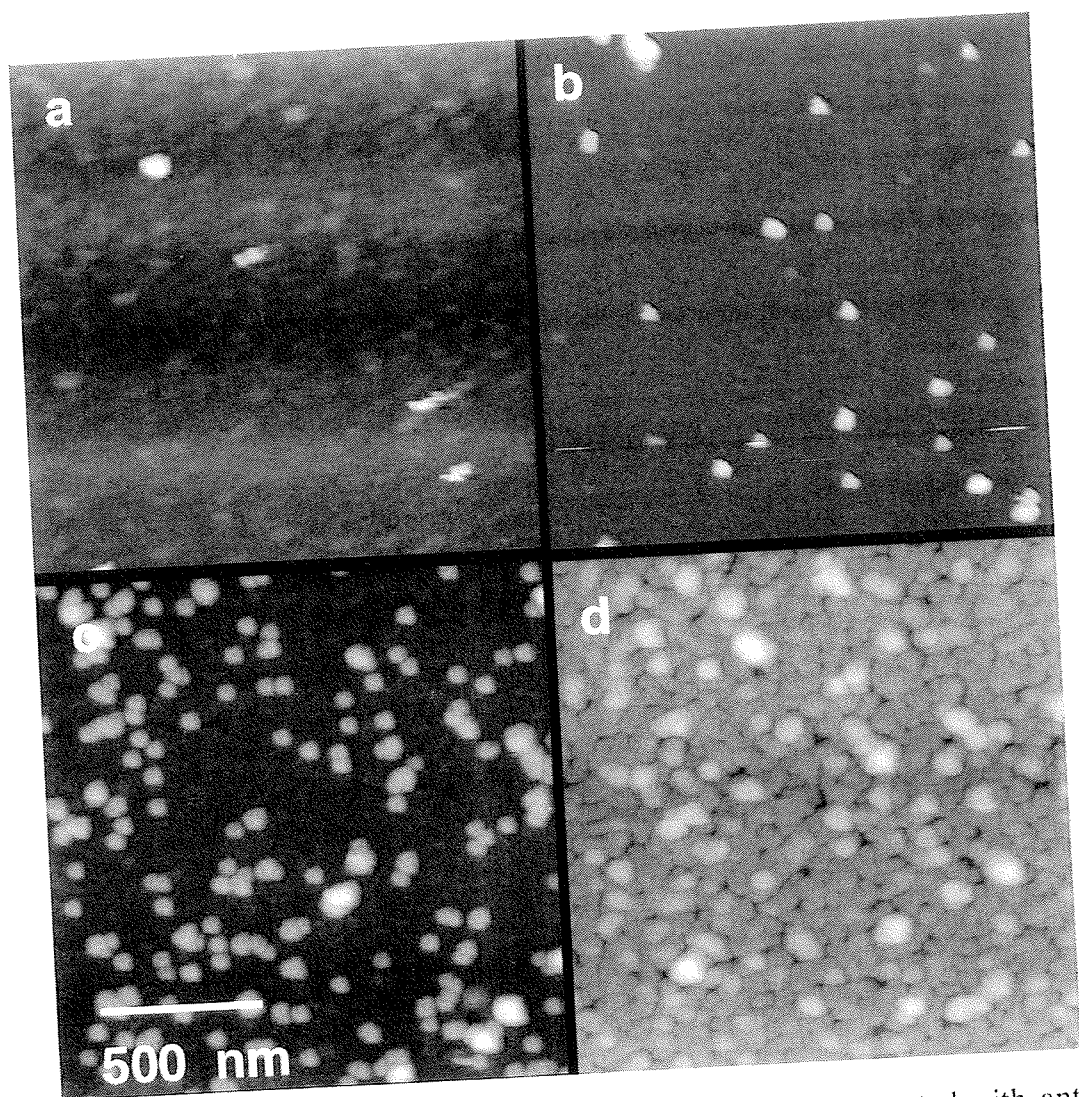


FIGURE 6. Successive increase in surface coverage of gold particles coated with anti-protein A antibodies on a protein A surface as measured by SFM.

coverage. The underestimation by the SFM might be explained by the finite size of the tip and/or by the finite force applied by the tip to the soft protein layers. On the other hand, the overestimation by the optical measurement may indicate that a linear relationship between sensor signal (coupling angle) and surface coverage, does not hold for low surface coverage. It has been recently discussed that at least for low surface coverage, a protein adlayer has to be treated as optically anisotropic because of preferential orientation of the biomolecules on the surfaces (Nellen & Lukosz, 1993). Such anisotropy could play a special role in the present case since the surface modification with protein A has been designed to orientate the bound h-IgG molecules directionally. The large deviations in the results from the two methods probably indicate that the observed sensor signals cannot be explained with a simple linear relationship between sensor signal and surface coverage. The results of this study therefore show that the direct SFM measurements can be employed in future to delineate the non-linear relationships that may exist at low surface coverages.

REFERENCES

- ALVAREZ-ICAZA, M. & BILITEWSKY, U. (1993) Mass production of biosensors. *Analytical Chemistry* **65**, 525A.
- ANSELMETTI, D., LÜTHI, R., MEYER, E., RICHMOND, T., DREIER, M., FROMMER, J. & GÜNTHERODT, H.-J. (1994) Attractive-mode imaging of biological materials with dynamic force microscopy. *Nanotechnology* **5**, 87–94.
- BAIN, C.D. & WHITESIDES, G.M. (1989) Attenuation length of photoelectrons in hydrocarbon films. *Journal of Physical Chemistry* **93**, 1670.
- BUTT, H.-J., WOLFF, E.K., GOULD, S.A.C., DIXON NORTHERN, B., PETERSON, C.M. & HANSMA, P.K. (1990) Imaging cells with the atomic force microscope. *Journal of Structural Biology* **105**, 54.
- CAMMANN, K., LEMKE, U., ROHEN, A., SANDER, J., WILKER, H. & WINTER, B. (1991) Chemo- und Biosensoren-Grundlagen und Anwendungen. *Angewandte Chemie* **103**, 519.
- DRAKE, B., PRATER, C.B., WEISENHORN, A.L., GOULD, S.A., ALBRECHT, T.R., QUATE, C.F., CANNELL, D.S., HANSMA, H.G. & HANSMA, P.K. (1989) Imaging crystals, polymers, and processes in water with the atomic force microscope. *Science* **243**, 1586.
- ESSERS, P. (1988) Principles in adsorption to polystyrene. *Nunc Bulletin* **6**.
- EXTRAND, C.W. & HESLOT, F. (1993) Experimental comparison between atomic force microscopy and ellipsometry on thin heterogeneous rubber films. *Journal of Vacuum Science and Technology* **11**, 112–114.
- GODING, J.W. (1978) Use of staphylococcal protein A as an immunological reagent. *Journal of Immunology* **20**, 241.
- HANSMA, H.G., BEZANILLA, M., ZENHAUSERN, F., ADRIAN, M. & SINSHEIMER, R.L. (1993) Atomic force microscopy of DNA in aqueous solutions. *Nucleic Acids Research* **21**, 505–512.
- HUBER, W., BARNER, R., FATTINGER, CH., HÜBSCHER, J., MÜLLER, F., SCHLATTER, D. & LUKOSZ, W. (1992) Direct optical immunosensing (sensitivity and selectivity). *Sensors and Actuators B* **6**, 122.
- KALLURY, K.M.R., THOMPSON, M., TRIPP, C.P. & HAIR, M.L. (1992) Interaction of silicon surfaces silanized with octadecylchlorosilanes with octadecanoic acid and octadecamine studied by ellipsometry, X-ray photoelectron spectroscopy, and reflectance Fourier transform infrared spectroscopy. *Langmuir* **8**, 947–954.
- KEIFER, E., RUDIN, W., BETSCHART, B., WEISS, N. & HECKERT, H. (1986) Demonstration of anti-cuticular antibodies by immuno-electron microscopy in sera of mice immunized with cuticular extracts and isolated cuticles of adult *Dipetalonema viteae* (Filarioidea). *Acta Tropica* **43**, 99.
- LUKOSZ, W. (1991) Principles and sensitivities of integrated optical and surface plasmon sensors for direct affinity sensing and immuno sensing. *Biosensors and Bioelectronics* **6**, 215.
- LUKOSZ, W. & TIEFENTHALER, K. (1988) Sensitivity of integrated and prism coupler as (bio)chemical sensors. *Sensors and Actuators* **15**, 273.
- LUKOSZ, W. & TIEFENTHALER, K. (1983) Embossing technique for fabricating integrated optical components in hard inorganic waveguiding materials. *Optics Letters* **8**, 537–539.

- NELLEN, PH. & LUKOSZ, W. (1993) Integrated optical input grating coupler as direct affinity sensors. *Biosensors and Bioelectronics* **8**, 129.
- LUONG, J.H.T., GROOM, C.A. & MALE, K.B. (1991) The potent role of biosensors in the food and drink industry. *Biosensors and Bioelectronics* **6**, 547.
- NUZZO, B.G., FUSCO, F.A. & ALLARA, D.L. (1987) Spontaneously organized molecular assemblies. Preparation and properties of solution adsorbed monolayers of organic disulfides and gold surfaces. *Journal of the American Chemistry Society* **109**, 2358.
- SCHLATTER, D., BARNER, R., FATTINGER, CH., HUBER, W., HÜBSCHER, J., HURST, J., KOLLER, H., MANGOLD, C. & MÜLLER, F. (1993) The difference interferometer: application as a direct affinity sensor. *Biosensors and Bioelectronics* **8**, 109.
- SCHMITT, F.-J., WEISENHORN, A.L., HANSMA, P.K. & KOLL, W. (1991) Interfacial recognition reactions as seen by fluorescence-, surface plasmon- and atomic force microscopies. *Makromolekulare Chemie Macromolecular Symposia* **46**, 133.
- SLOT, J.W. & GEUZE, H.J. (1985) A new method of preparing gold probes for multiple-labeling cytochemistry. *European Journal of Cell Biology* **38**, 87.
- THOMPSON, H. & KRULL, U.J. (1991) Biosensors and the transduction of molecular recognition. *Analytical Chemistry* **63**, 393A.
- TILLMAN, N., ULMAN, A., SCHILDKRAUT, J.S. & PENNER, T.L. (1988) Incorporation of phenoxy groups in self assembled monolayers of trichlorosilane derivatives: effects on film thickness, wettability and molecular orientation. *Journal of the American Chemistry Society* **110**, 6163.
- ULMAN, A., EILERS, J.E. & TILLMAN, N. (1989) Packing and molecular orientation of alkanethiol monolayers and gold surfaces. *Langmuir* **5**, 1147.
- ULMAN, A. (1990) Self assembled monolayers of alkyltrichlorosilanes: building blocks for future organic materials. *Advanced Materials* **2**, 573.
- WEISENHORN, A.L., EGGER, E., OHNESORGE, F., GOLILD, S.A.C., HEYN, S.P., HANSMA, H.G., SINSHEIMER, R.L., GAUB, H.E. & HANSMA, P.K. (1991) Molecular-resolution images of Langmuir-Blodgett films and DNA by atomic force microscopy. *Langmuir* **7**, 8–12.